Audio Engineering Society

Convention Paper 9977

Presented at the 144th Convention
2018 May 23 – 26, Milan, Italy

Surround with Depth on First-Order Beam-Controlling Loudspeakers

Thomas Deppisch[1,2], Nils Meyer-Kahlen[1,2], Franz Zotter[2,3], and Matthias Frank[2,3]

[1] *University of Technology, Graz, Austria*
[2] *University of Music and Performing Arts, Graz, Austria*
[3] *Institute of Electronic Music and Acoustics*

Correspondence should be addressed to Thomas Deppisch (thomas.deppisch@student.tugraz.at)

ABSTRACT

Surround systems are typically based on fixed-directivity loudspeakers pointing towards the listener. Laitinen et al. showed for a variable-directivity loudspeaker that directivity control can be used to influence the distance impression of the reproduced sound. As we have shown in a listening experiment, using beam-controlling loudspeakers, stable auditory events at directions additional to the loudspeaker positions can be created by exciting specific wall reflections. We use these two effects to enable distance control and increase the number of effective surround directions in two different surround setups. We present IIR filter design derived from a physical model, which achieves low frequency beam-control for our novel cube-shaped 4-channel loudspeakers.

1 Introduction

Other than standard surround setups, see e.g. ITU BS2051, the proposed surround-with-depth system uses first-order variable-directivity loudspeakers to enhance surround sound playback in different configurations. While in Poletti et al. [1], reflections are suppressed to enhance sound field reproduction with third-order cylindrical loudspeakers, what we present explicitly excites reflections to create additional auditory cues. We demonstrate that wall reflections are helpful in creating auditory events at other locations than the loudspeaker cubes' positions, and evaluate this in a listening experiment. This has already been studied for the icosahedral loudspeaker (IKO) [2].

While the IKO is able to control third-order directivity patterns, our listening experiment indicates that also first-order systems are capable of utilizing the wall reflections. Audio electronics exploits the principle in sound bars, where surround signals are created by a single loudspeaker array generating beams steered towards the walls and ceiling, see e.g. [3].

What is more, the perceived distance of an auditory event can be controlled by varying loudspeaker directivity, as shown by Laitinen et al [4]. A change in direct-to-reverberant energy ratio (D/R-ratio), which is caused by turning the main beam direction away from the listener, is able to evoke an increased perceived distance.

Fig. 1: Surround-with-depth setup with 4 loudspeaker cubes (4 channels each).

For the realization of the surround-with-depth method, the use of cubical loudspeaker arrays (cf. Fig. 1) is proposed, whose four transducers point to each of the four cardinal directions. These allow for controlling first-order directivity-patterns with arbitrary shapes and directions in the horizontal plane by superimposing a monopole and two orthogonal dipole basis patterns. In this contribution, we refer to the engineering brief [5] for the construction and measurement details of the cube loudspeakers. We discuss the electroacoustic properties of the loudspeakers in their cubical housing, which is necessary to equalize monopole and dipole directivity patterns. To describe analytic equalization filters, the discussion is based on the Thiele/Small parameters describing mechanical and electromechanical parts of the transducers, the interior impedance coupling of the loudspeakers, and the exterior radiation transfer functions. Furthermore, discrete-time domain filters based on the corrected impulse invariance technique are derived.

In section 2 we describe the creation of first-order directivity patterns. The physical model and the resulting IIR filters are presented in section 3, followed by the surround-with-depth approach and the effects it is based in section 4. Section 5 presents a listening experiment, which validates the effectiveness of stabilizing an auditory event via the excitation of wall reflections by two sound beams. In section 6 an implementation as open source DAW plug-in is provided.

2 Creating First-Order Directivity Patterns

A first-order directivity pattern of the form

$$D(\varphi) = \underbrace{(1-\alpha)}_{\text{omnidirectional}} + \underbrace{\alpha\ \cos(\varphi-\varphi_0)}_{\text{figure-of-eight}} \tag{1}$$

points towards the angle φ_0 and has a variable shape, which can be controlled continuously by the parameter α, where $\alpha = 0$ corresponds to an omnidirectional loudspeaker directivity, $\alpha = 0.5$ to a cardioid-shaped and $\alpha = 1$ to a figure-of-eight-shaped directivity.

Such a pattern can be created by superimposing a monopole basis pattern with a scalable amount of two orthogonal dipole patterns. The monopole signal needs to be weighted with $(1-a)$ and the orthogonal dipole patterns with $\alpha\ \cos(\varphi_0)$ and $\alpha\ \sin(\varphi_0)$ respectively. This principle of superposition is known from Double-MS in microphone technology, where one omnidirectional and two figure-of-eight microphones are combined to create a variable pickup pattern. In case of the cube-shaped loudspeaker the monopole basis pattern is formed by all four loudspeaker drivers playing in-phase, while the dipole basis pattern is created by two opposing drivers playing out-of-phase as depicted in Fig. 2.

The frequency response of the radiated sound pressure due to monopole and dipole excitation differs at low frequencies (cf. Fig. 3b). To create controllable directivity patterns, we need to equalize the responses with respect to each other.

3 From Physical Model to IIR Filters

To obtain simple analytic filter curves equalizing the radiated modes, we model its electroacoustic subsystems: voltage to transducer force, suspension and mass of the loudspeaker cone, interior acoustic coupling, and radiation. Every transducer consists of electrical, electromechanical, and mechanical subsystems, described by the Thiele/Small parameters as constants specified in the loudspeaker's data sheet, cf. Tab. 1.

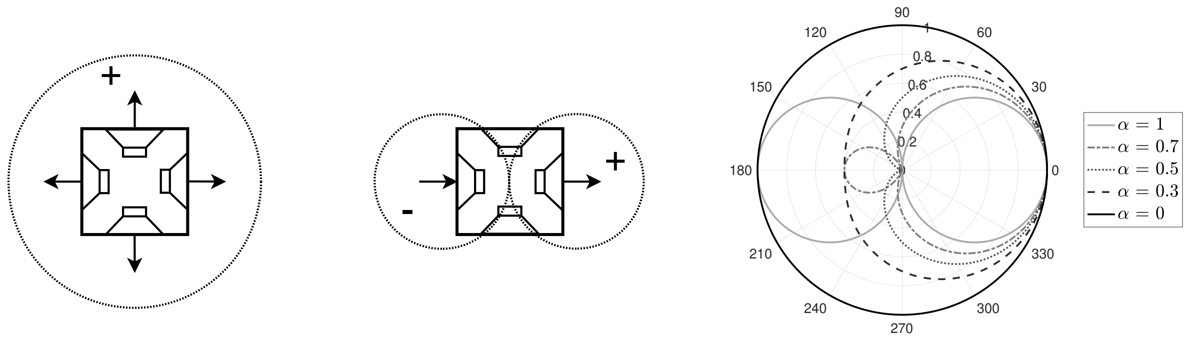

(a) **(b)** **(c)**

Fig. 2: (a) Monopole synthesis by 4 loudspeakers in-phase. (b) Dipole synthesis by opposing loudspeakers out-of-phase. (c) Resulting ideal directivity $D(\varphi) = (1-\alpha) + \alpha\ \cos(\varphi - \varphi_0)$ for varied α.

DC coil resistance	R	3.2	Ω
Coil inductance	L	0.6	10^{-3}H
Force factor	Bl	4.4	Tm
Effective piston area	A	129	10^{-4}m^2
Dynamically moved mass	M	12	10^{-3}kg
Equivalent volume	V_m	38	10^{-3}m^3
Mechanical Q factor	Q_m	2.16	

Table 1: Thiele/Small parameters from the datasheet, naming complies with the model description.

The stiffness S_m of the loudspeaker cone's suspension is obtained from the equivalent volume V_m, effective piston area A, density of air $\rho = 1.2$ kg/m^3 and the speed of sound $c = 343$ m/s

$$S_\mathrm{m} = \frac{\rho c^2 A^2}{V_\mathrm{m}} = 618\,\mathrm{N/m}. \tag{2}$$

Its friction losses are calculated from the mechanical Q factor Q_m and the dynamically moved mass M

$$R_\mathrm{m} = \frac{\sqrt{M S_\mathrm{m}}}{Q_\mathrm{m}} = 1.26\,\mathrm{Ns/m}. \tag{3}$$

Electroacoustic model. In the Laplace s-domain ($s = \mathrm{i}\omega$), the input voltage U_i of the i^th electrodynamic loudspeaker consists of voltages $R I_i$ and $s L I_i$ to drive the current I_i through resistance and inductance of the coil plus the induced voltage $U_{\mathrm{ind},i}$ of the moving coil

$$U_i = \underbrace{(R + Ls)}_{Z_\mathrm{c}} I_i + U_{\mathrm{ind},i}\ , \tag{4}$$

with the static-coil impedance Z_c. The current I_i moreover produces a mechanical force F_i acting on the loudspeaker cone, which is proportional to the transduction constant Bl, which also relates velocity v_i to induced voltage $U_{\mathrm{ind},i}$

$$F_i = Bl\, I_i, \qquad U_{\mathrm{ind},i} = Bl\, v_i. \tag{5}$$

Mechanically, a force F_i is required to drive the loudspeaker cone with the velocity v_i. It subdivides into the forces $s M v_i$ to drive the cone's mass, $S_\mathrm{m}\, v_i\, s^{-1}$, and $R_\mathrm{m}\, v_i$ to overcome stiffness and friction losses of the suspension, plus the exterior acoustical force $F_{\mathrm{a},i}$ acting on the cone

$$F_i = \underbrace{(M s + R_\mathrm{m} + S_\mathrm{m} s^{-1})}_{Z_\mathrm{m}}\, v_i + F_{\mathrm{a},i}\ , \tag{6}$$

where Z_m denotes the impedance in vacuum. While the above equations hold without coupling between the loudspeakers, $i = 1, \ldots, 4$, the acoustical force $F_{\mathrm{a},i} = \sum_{j=1}^{4} Z_{\mathrm{a},ij}\, v_j$ couples the loudspeakers' movements over the enclosed air of the common housing. At high frequencies, the impedance sM will dominate the force F_i and acoustic coupling of higher interior modes becomes irrelevant. The coupling is sufficiently well modeled by the 0 Hz compression mode to which the sum of all velocities contribute, multiplied with stiffness S_a of the enclosed air

$$F_{\mathrm{a},i} = \underbrace{\overbrace{\frac{\rho c^2 A^2}{V}}^{S_\mathrm{a}}\, s^{-1}}_{Z_\mathrm{a}} \sum_{j=1}^{4} v_j\ , \tag{7}$$

yielding the impedance Z_a. As seen from equation 7, the acoustical coupling is non-zero only for the monopole.

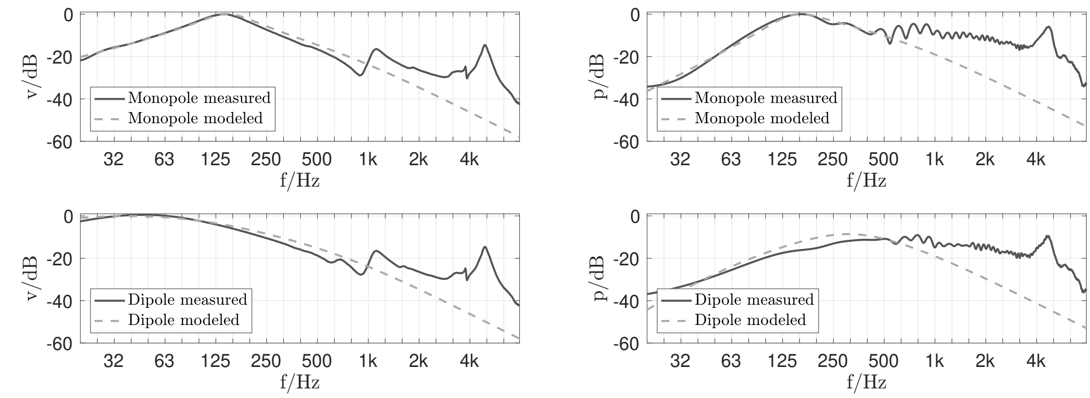

(a) **(b)**

Fig. 3: Comparison of the physical model against measurement for monopole and dipole pattern, (a) loudspeaker driver velocity and (b) radiated sound pressure with the measurement averaged in the horizontal plane.

Input voltages to output velocities, verification. The velocities of the four cones of the loudspeaker cube determine how much sound is going to be radiated. From the above equations, we establish the relation between input voltage U and output velocity v as

$$\begin{aligned} U_i &= Z_c Bl^{-1} F_i + Bl\, v_i \\ &= Z_c Bl^{-1} \left(Z_m\, v_i + Z_a \textstyle\sum_{j=1}^{4} v_j\right) + Bl\, v_i. \end{aligned} \tag{8}$$

The *monopole mode* is driven with all-equal velocities of the loudspeakers $v_i = v$. Inserted, this yields the required voltage $U_{\mathrm{mon}} = [Z_c Bl^{-1} (Z_m + 4Z_a) + Bl]v$ for every loudspeaker $U_i = U_{\mathrm{mon}}$, see Fig. 4.

The *dipole mode* is driven with opposing loudspeakers out of phase, e.g. $v_1 = -v_3 = v$ and $v_2 = v_4 = 0$, which yields the required voltage $U_{\mathrm{dip}} = [Z_c Bl^{-1} Z_m + Bl]v$ for the pair $U_1 = -U_3 = U_{\mathrm{dip}}$ while the others are mute.

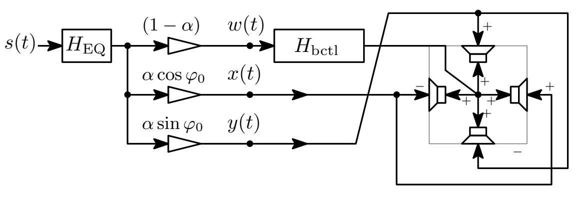

Fig. 4: Signal flow diagram showing the adjustable parametric master equalizer H_{EQ}, O/8 balance with α, beam direction φ_0, monopole-to-dipole equalizer H_{bctl} and monopole and dipole mode control.

These transfer functions are used to verify the electroacoustic model by input voltages to output velocities measurements from [5] as shown in Fig. 3a. In the frequency range below 1 kHz the loudspeaker moves as one rigid part and complies with the model.

Velocities to radiated sound pressure. In the next step, far field radiation properties of the two basis patterns are added to the model to incorporate the change in the frequency response when undergoing radiation. Spherical Hankel functions of the second kind $h_n^{(2)}$ and their derivatives $h_n'^{(2)}$ are solutions for the radial component of the wave equation evaluated in spherical coordinates [6]. They are used to translate an n^{th} order spherical wave spectrum for particle velocity at radius r_0 to a spherical wave spectrum for sound pressure in far field. If spatial aliasing above 1 kHz is disregarded for now, the monopole mode primarily excites the omnidirectional, zeroth-order beam pattern, and the dipole modes primarily excite the corresponding figure-of-eight, first-order beam patterns. Hence, the spherical wave spectra radiation characteristics apply, yielding

$$H_n = \frac{\rho c\, \mathrm{i}^{n+1}}{k\, h_n'^{(2)}(s, r_0)} \tag{9}$$

as the transfer function of the n^{th} order basis pattern from radius r_0 to far field in the Laplace domain. The resulting radiation characteristics are validated by measurement as shown in Fig. 3b. All the measurement data used in this paper is provided online[1].

[1] `http://phaidra.kug.ac.at/o:67631`

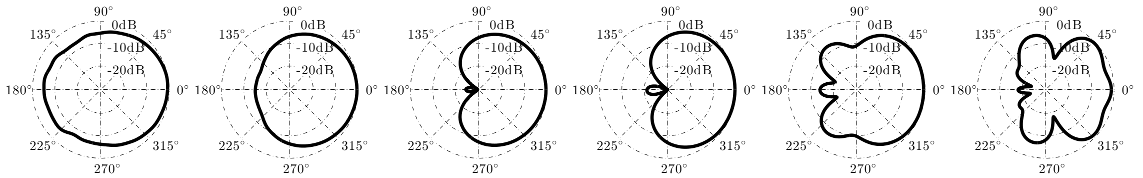

(a) 63 Hz (b) 125 Hz (c) 250 Hz (d) 500 Hz (e) 1 kHz (f) 2 kHz

Fig. 5: Plots for cardioid-shaped directivity patterns ($\alpha = 0.5$) after monopole equalization for frequencies from 63 Hz to 2 kHz.

Monopole-to-dipole equalizer. Instead of equalizing both the monopole and dipole driving voltages $[U_{\mathrm{mon}}, U_{\mathrm{dip}}]$, it is more convenient to apply equalization only to the monopole voltage by using $[U_{\mathrm{mon}}/U_{\mathrm{dip}}, 1]$. The filter $H_{\mathrm{eq1}} = \frac{U_{\mathrm{mon}}}{U_{\mathrm{dip}}}$ to equalize the monopole velocities to those of the dipoles is

$$H_{\mathrm{eq1}} = \frac{\left[M s + R_{\mathrm{m}} + (S_{\mathrm{m}} + 4 S_{\mathrm{a}})\, s^{-1}\right](R + L s) + (Bl)^2}{\left[M s + R_{\mathrm{m}} + S_{\mathrm{m}}\, s^{-1}\right](R + L s) + (Bl)^2}. \tag{10}$$

By compensating for the monopole radiation transfer function H_0 and applying dipole radiation characteristics H_1 (cf. Eq. 9) we define the far field radiation control filter

$$\begin{aligned} H_{\mathrm{eq2}} = \frac{H_1}{H_0} &= \frac{\mathrm{i} h_0^{\prime(2)}(s, r_0)}{h_1^{\prime(2)}(s, r_0)} \\ &= \frac{[s + (c/r_0)]\, s}{s^2 + 2(c/r_0)\, s + 2(c/r_0)^2}\ , \end{aligned} \tag{11}$$

where the effective radius $r_0 = 24$ cm was used in case of the cubical loudspeakers. With both the far field radiation control H_{eq2} and the monopole-to-dipole equalizer H_{eq1}, we equalize the monopole input voltage by $H_{\mathrm{bctl}} = H_{\mathrm{eq1}} H_{\mathrm{eq2}}$ to produce far field radiation equalized in magnitude and phase. This equalization is effective in a frequency range from approximately 100 Hz to 1 kHz and is validated by measurement as shown in the resulting directivity plots in Fig. 5.

Discrete-time implementation by impulse invariance. By sampling a continuous-time impulse response $h(t)$ at discrete times $t = nT$, with the sampling period $T = 1/f_{\mathrm{s}}$ and sample index $n = 0, 1, 2, \ldots$, one obtains an impulse-invariant discrete-time impulse response $h[n] = T\, h(nT)$. As outlined in [7], with corrections by Jackson [8], Mecklenbräuker [9] and Eitelberg [10], one can split any transfer function of equal-order numerator and denominator into a freqency-independent throughput K and a strictly proper low pass H_{lp} in the Laplace s domain, yielding

$$H(s) = K + H_{\mathrm{lp}}(s). \tag{12}$$

The discrete-time impulse response samples the low-pass response $h_{\mathrm{lp}}(t)$ at $t = nT$, removes half of the sample at the instant $n = 0$, and adds the throughput K

$$h[n] = K\left[\delta[n] - \frac{T}{2} h_{\mathrm{lp}}(0)\delta[n]\right] + T\ h_{\mathrm{lp}}(nT). \tag{13}$$

Application of the corrected impulse invariance yields discrete-time filters shown in Fig. 6, matching the Laplace-domain filters (eq. 10, 11) very well in magnitude and phase. A Matlab implementation for calculating the Laplace domain filters for given Thiele/Small parameters and retrieving the discrete-time filters via the corrected impulse invariance is provided online[2].

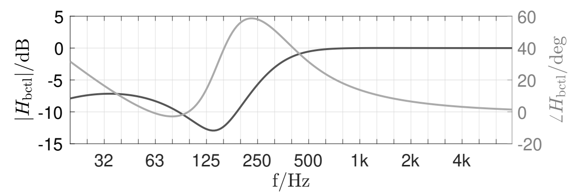

Fig. 6: Magnitude response (black) and phase response (grey) of the combined equalizer filter H_{bctl}.

4 Surround-with-Depth Setup

Placing one of the described 4-channel cubical loudspeakers in a room corner, we use three meaningful beam constellations (cf. Fig. 7): (i) directly towards the listener as in a usual stereo setup, (ii) in the opposing direction away from the listener towards the room corner and (iii) directed to one of the sides, causing a perceivable reflection on the respective wall.

[2] https://opendata.iem.at

The full surround-with-depth setup with four loudspeakers arranged in a rectangle makes use of these three different kinds of beams to form a quadraphonic system, which has smooth panning, a large sweet spot and additional distance control.

When fading over between the direct (1) and the corner-facing beam (2), the change in D/R-ratio yields a change of the perceived distance [4] establishing the distance control. Reflections caused by sideways-steered beams (3) can be perceived as separate auditory events giving the opportunity to use reflections as additional virtual loudspeakers to stabilize panning. Such created auditory events are especially stable when using two reflections between a loudspeaker pair, as shown in a listening experiment in section 5.

Thus, for panning we have eight positions available: Four real loudspeaker positions created by direct beams and four reflected-sound virtual loudspeakers, each created by two beams (cf. Fig. 7). Continuous circular panning on this ring is achieved by using third-order max-r_E weighted, horizontal Ambisonic panning [11]. The additional distance control is enabled by fading over from this ring to a second diffuse layer formed by the beams playing towards the corners, for which only first-order Ambisonics is required.

The use of supercardioid beam patterns for the inner third-order panning circle and cardioid-shaped beam patterns for the outer first-order circle accomplishes to steer the zeros of the corresponding pattern towards the direction of the listener and thus minimizing the crosstalk due to the pattern's sidelobes.

5.1 Setup. A second setup is designed for playing back standard 5.1 surround material with two beam-controlling loudspeakers. While the left and right channels are played back conventionally with a directivity pattern pointing directly towards the listener, the center channel is projected as a reflected-sound virtual source on the wall. The left and right surround channels are played back using cardioid-shaped beams steered to the left and the right wall.

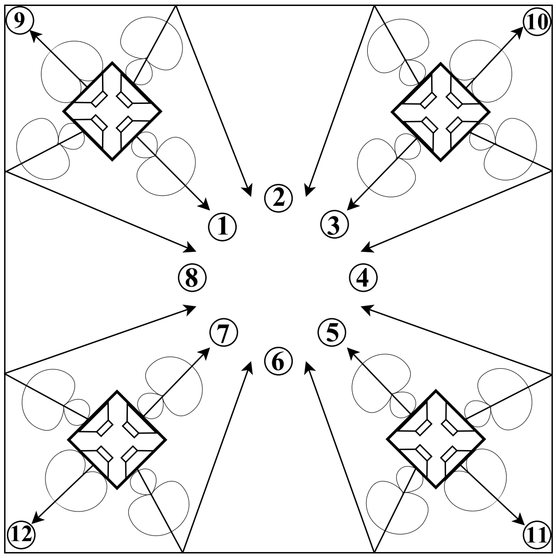

Fig. 7: Surround-with-depth setup with 4 loudspeaker cubes for third-order horizontal Ambisonic panning on 4 direct beams (1, 3, 5, 7) plus 4 reflected-sound directions (2, 4, 6, 8), blended with 1st order horizontal Ambisonic panning to 4 indirect beams to the room corners (9, 10, 11, 12) for controllable distance.

5 Listening Experiment: Virtual Loudspeakers

To show in which way a quadraphonic setup of the loudspeaker cubes effectively produces a stable center auditory event created between each pair, we carried out a listening experiment to determine the sweet area. The sweet area is bounded by the lateral distance left and right from the middle, at which the auditory event leaves a target localization range of 1.4 m (cf. Fig. 8a). 15 listeners took part in the experiment and were asked to write down the boundaries of the sweet area along two lines (A) and (B) at two listening distances from the pair of loudspeaker cubes as shown in Fig. 8a. For a listener in the middle of line A the loudspeakers appear at angles $\pm 45°$, which would correspond to the ideal listening position in classic quadraphonics. In the middle of line B, the loudspeakers are located at approximately $\pm 30°$, as in ideal stereo playback.

There were four ways of presentation for the center auditory image: (i) by a beam pair from the left and right loudspeaker cube, both aiming at the center listening spot, (ii) by both loudspeaker cubes playing omnidirectionally, (iii) by one front-wall reflection excited by a beam from the left loudspeaker cube, and (iv) by a pair of front-wall reflections excited by a beam from both the left and the right loudspeaker cubes.

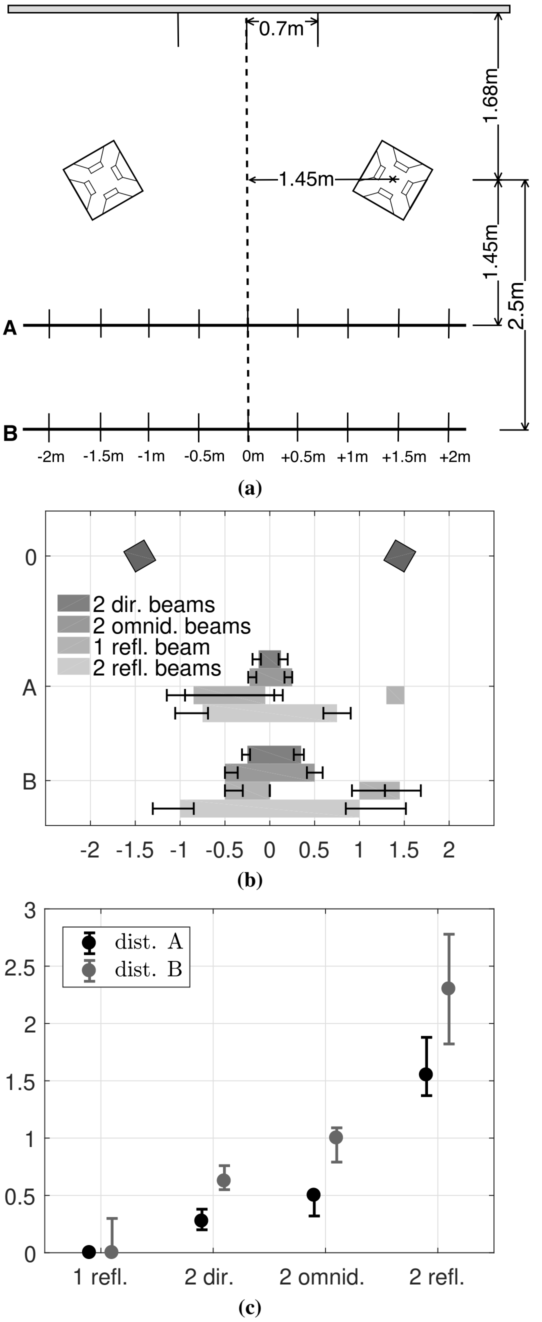

Fig. 8: Geometry of the experimental setup (a) with ticks on lines A and B used by subjects to indicate boundaries of both sweet lines, in which the auditory event stays between ±0.7 m, (b) resulting median-to-median lengths for different conditions and their 95%-confidence intervals, (c) individual lengths given for both sweet lines under 4 different conditions.

Each listener was presented the four conditions with male speech [12] twice in a random sequence, and was asked for each condition to write down the both boundaries of the sweet line. Listeners started with the 8 responses for the listening distance on line A and proceeded with their 8 responses on line B.

Results. A Kruskal-Wallis test comparing all conditions pair-wise yields that all conditions lead to significantly different sweet area lenghts ($p < 0.05$), see also 95%-confidence intervals shown in Fig. 8c. The listening experiment clearly shows that the smallest sweet area can be expected from a single first-order beam reflected at the front wall, condition (iii). Such a beam causes two small sweet areas which are not centered (cf. Fig. 8b), and more than half of the listeners (12 for A, 8 for B) reported there being no useful localization at all. Condition (i) with a cardioid-shaped beam pair oriented to the central listening spot from each cube yields a significantly larger sweet area ($p < 0.05$) than (iii). Condition (ii) with omnidirectional radiation from both cubes yields a significantly wider sweet area than the direct beam pair of (i), and despite it more strongly excites the room and diffuse field as well, the indirect beam pair (iv) exciting two front-wall reflections by a beam from each cube yields the significantly largest sweet area, whose length of 2.3 m nearly covers all the basis length 2.9 m of the pair of loudspeaker cubes at the listening distance B at 2.5 m.

We conclude that despite a quadraphonic loudspeaker setup with loudspeakers at $\pm 45°$ and $\pm 135°$ would not give highly stable localization results [13], a quadraphonic layout built from beam-controlling loudspeaker cubes can, when involving the surrounding walls into the playback via reflections.

6 Plug-In Implementation

To establish surround-with-depth playback, audio plug-ins for use in a digital audio workstation (DAW) were developed using the C++ framework JUCE[3]. They work under any DAW that is able to host multi-channel tracks of either 16 channels (*CubesSurroundDecoder*) or 8 (*Cubes5.1Player*). The plug-ins are released under the open source GNU GPLv3 license and are available online[4].

[3] https://juce.com/

[4] https://git.iem.at/audioplugins/CubeSpeakerPlugins

CubesSurroundDecoder. A DAW working environment for the first setup consisting of four cube loudspeakers is set up by placing the *DistanceEncoder* plug-in (cf. Fig. 9a) on any mono audio track to be played back. By dragging the white dot along the circle, the mono input is placed at the corresponding surround panning angle. By adjusting the distance knob to any value between 0 and 1, the distance effect is controlled, yielding perceptually proximal signals for the value 0 and maximally distant ones for 1.

The encoded signals are sent to a decoding bus, where the *CubesSurroundDecoder* (cf. Fig. 9b) creates a 16-channel output signal supplying the four cubes. The GUI symbolizes each of the four loudspeaker cubes by a rectangle surrounded by a circle. On each of these circles, the directions of four sound beams can be adjusted to fit the geometry of the playback environment; dragging the white dots labeled by the letters F, L, R and B controls the beam directions of the front, left, right and backward-facing beams.

The gains of the direct (F/Direct), side (L,R/Sides) and backward-facing beams (B/Diffuse) as well as a high shelf gain for the side beams (HS) are adjusted by separate gain controls on top. The directivity parameter α is controlled by the "O/8 balance" knobs at the bottom. Moreover, the plug-in offers a three-band equalizer to customize the overall sound.

Somewhat more special, a delay knob on the bottom-right permits to delay the signals of the front beams (F) relative to the side (L,R) and back beams (B). A switch at the bottom of the plug-in toggles the dipole equalization filters explained in section 3. At high frequencies, the modal beamforming can be replaced by a more effective pairwise beamforming using Vector-Base Amplitude Panning (VBAP) [14].

Cubes5.1Player. To play back 5.1 audio material using the second setup described above, the *Cubes5.1Player* plug-in needs to be put on a 8-channel audio track. The structure of the plug-in is similar to the *CubesSurroundDecoder* with the difference that only two cube loudspeakers are involved.

7 Conclusion

We presented a novel surround-with-depth approach and the underlying principles. We described and verified the design of a first-order beam control for cube-shaped loudspeakers by modeling their physical properties. Our verification used measurements of the loudspeaker cone velocities and the radiated sound pressure.

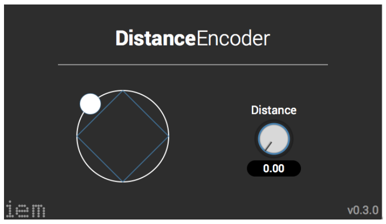

(a)

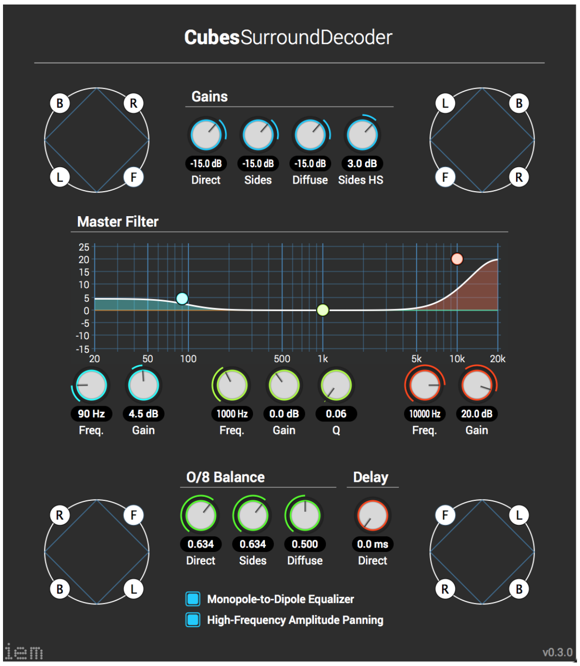

(b)

Fig. 9: (a) *DistanceEncoder* plug-in to be put on a mono audio track for encoding of direction and perceived distance and (b) *CubesSurroundDecoder* plug-in for decoding to the 16 hardware channels of four loudspeakers.

Moreover, we derived discrete-time filters to equalize the electroacoustic and radiation properties of the monopole with respect to the dipole pattern. Directivity plots show that accurate beam control is achieved below 1 kHz.

We described the two perceptual phenomena on which the surround-with-depth approach is based: (i) manipulation of the distance impression by direct to reverberant control, and (ii) more stable auditory events between the loudspeakers by explicit beam control towards wall reflections.

A listening experiment provided evidence that such additional auditory events created by two sound beams are perceived in the center within an enlarged sweet area compared to standard stereo and quadraphonic setups. The measurement data and Matlab scripts to calculate discrete-time filters for arbitrary Thiele/Small parameters are provided and can be used to equalize self-built cubical loudspeakers. Open source DAW plug-ins were developed to produce and control playback.

References

[1] Poletti, M. A., Betlehem, T., and Abhayapala, T. D., "Higher-Order Loudspeakers and Active Compensation for Improved 2D Sound Field Reproduction in Rooms," *J. Audio Eng. Soc*, 63(1/2), pp. 31–45, 2015.

[2] Wendt, F., Frank, M., Zotter, F., and Höldrich, R., "Directivity Patterns Controlling the Auditory Source Distance," in P. Rajmicand, F. Rund, and J. Schimmel, editors, *Proceedings of the 19th International Conference on Digital Audio Effects (DAFx-16)*, ACM, 2016, ISSN 2413-670.

[3] Takumai, S., "Loudspeaker Array Device and Method For Setting Sound Beam of Loudspeaker Array Device," WIPO patent WO 2,006,001,272 A1, 2006, filed 21 June 2005, and granted 5 January 2006.

[4] Laitinen, M.-V., Politis, A., Huhtakallio, I., and Pulkki, V., "Controlling the perceived distance of an auditory object by manipulation of loudspeaker directivity," *The Journal of the Acoustical Society of America*, 137(6), pp. EL462–EL468, 2015, doi:10.1121/1.4921678.

[5] Meyer-Kahlen, N. and Pollack, K., "Design and Measurement of First-Order, Horizontally Beam-Controlling Loudspeaker Cubes," in *144th AES Conv. Milano*, 2018.

[6] Williams, E. G., *Fourier Acoustics*, Academic Press, 1999.

[7] Pomberger, H., *Angular and Radial Directivity Control for Spherical Loudspeaker Arrays*, Diploma thesis, University of Music and Performing Arts, Graz, 2008.

[8] Jackson, L. B., "A correction to impulse invariance," *IEEE Signal Processing Letters*, 7(10), pp. 273–275, 2000, ISSN 1070-9908, doi:10.1109/97.870677.

[9] Mecklenbräuker, W. F., "Remarks on and correction to the impulse invariant method for the design of IIR digital filters," *Signal Processing*, 80(8), pp. 1687 – 1690, 2000, ISSN 0165-1684, doi:https://doi.org/10.1016/S0165-1684(00)00113-4.

[10] Eitelberg, E., "Convolution invariance and corrected impulse invariance," *Signal Processing*, 86(5), pp. 1116 – 1120, 2006, ISSN 0165-1684, doi:https://doi.org/10.1016/j.sigpro.2005.11.003.

[11] Frank, M., Zotter, F., and Sontacchi, A., "Localization Experiments Using Different 2D Ambisonics Decoders," in *25th Tonmeistertagung – VDT International Convention*, 2008.

[12] EBU, "EBU SQAM CD Sound Quality Assessment Material recordings for subjective tests," 2008.

[13] Ratliff, P. A., "Properties of hearing related to quadraphonic reproduction," *BBC R&D Report*, 1974.

[14] Pulkki, V., "Virtual Sound Source Positioning Using Vector Base Amplitude Panning," *J. Audio Eng. Soc*, 45(6), pp. 456–466, 1997.